Electron-photon coincidence parameters for the $4s'[1/2]_1^0(^1P_1)$ and $4s[3/2]_1^0(^3P_1)$ states of argon

F. J. da Paixão*
Instituto de Fisica Gleb Wataghin, Universidade Estadual de Campinas, 13100 Campinas, São Paulo, Brazil

N. T. Padial†
Joint Institute for Laboratory Astrophysics, University of Colorado and National Bureau of Standards, Boulder, Colorado 80309

G. Csanak
Los Alamos National Laboratory, Los Alamos, New Mexico 87545
(Received 27 February 1984)

First-order many-body theory has been used to calculate electron-photon coincidence parameters for the $4s'[\frac{1}{2}]_1^0(^1P_1)$ and $4s[\frac{3}{2}]_1^0(^3P_1)$ states of argon, for the incident electron energies of 16, 20, 30, 50, and 80.4 eV. Consequences of the spin-orbit coupling in the target atom upon the interpretation of electron-photon coincidence experiments are discussed.

I. INTRODUCTION

The radiation following electron-impact excitation has an anisotropic intensity distribution and is polarized due to the preferred direction of the exciting electron beam. In the early experiments of Skinner,[1] Skinner and Appleyard,[2] and others, the angular distribution and polarization characteristics of the radiation after electron-impact excitation were studied.[3] The theory was initially developed by Oppenheimer[4-6] and Penney[7] and extended by Percival and Seaton.[8] They showed that information about the magnetic-sublevel integral cross sections for the level excited by the electrons could be obtained from the experiments. Electron-photon coincidence experiments (EPCE) are a refinement of this technique.[9]

Imhoff and Read[10] suggested that electrons be detected in the forward direction in coincidence with the emitted photons in order to simulate a "threshold excitation" situation; this experiment was later performed by King *et al.*[11] Pochat *et al.*[12] used the coincidence technique to measure the relative differential cross sections for the excitation of one level which strongly overlaps another. The most common theoretical analysis of EPCE comes from the works of Rubin *et al.*,[13] Macek and Jaecks,[14] and Wykes.[9] They showed that direct information about the scattering amplitudes can be obtained from EPCE. This experiment was later performed by Eminyan *et al.*[15,16] In this case, the observed radiation comes only from atoms that scattered the electron in a well-defined direction. The Macek-Jaecks formulation was used to extract two parameters λ and χ from their experiment on the 2^1P excitation on He. The calculation of these parameters, which are defined, respectively, as the ratio of the differential cross sections for the magnetic sublevels and as the relative phase of the scattering amplitude for the magnetic sublevels, provides a stringent test of the validity of theoretical models. Another method was used by Standage and Kleinpoppen,[17] who measured the Stokes parameters of the light emitted in the $3^1P\rightarrow 2^1S$ decay of He in coincidence with the scattered electrons.

A large number of EPCE were performed for various levels of helium,[18-31] neon,[19] argon,[32-34] krypton,[35-38] mercury,[39-41] sodium,[42] the hydrogen atom[43-48] and molecule,[49] and the nitrogen molecule.[50] The experimental situation up to 1979 has been reviewed by McConkey.[51]

For the general case, Fano and Macek[52] introduced four quantities, the alignment and orientation parameters, which separate geometrical and dynamical effects and are averages over the density matrix of the ensemble of excited atoms created by the collision and selected by the coincidence circuit. In the pure *LS*-coupled case, these parameters are not independent and can be expressed as functions of only two parameters, for example λ and χ. Blum and Kleinpoppen[53] reformulated the theory in a scheme that uses the density matrix[54] in a more transparent way.

The experiments have been conducted in one of two ways: (i) in the *electron-photon angular-correlation* experiments, the electron scattering angle is fixed and the number of coincidences per unit time are counted for a whole range of the photon-detector angles, irrespective of the spin of the electron and of polarization of the detected photon and (ii) in the *electron-photon polarization-correlation* experiments the coincidence rate is measured at a fixed photon-detector angle and the polarization characteristic, such as angle of linear polarization and direction of circular polarization, are changed. The incident electron beam is unpolarized, and there is no spin analysis of the scattered electrons. The theory for the case in which the incident electron beam is polarized has been formulated by Bartschat *et al.*[55] In addition, Macek and Hertel[56] showed that the Fano-Macek orientation and alignment parameters can also be obtained from experiments measuring superelastic electron scattering by laser-excited atoms. Thus, the interpretation of these experiments is also affected by our analysis.

In the present study we investigate some of the consequences of spin-orbit coupling in the target atom upon the Fano-Macek orientation and alignment parameters and, in general, upon the interpretation of electron-photon coincidence experiments. We shall discuss parameters[57] that are equivalent to those of Fano and Macek but which show the spin-orbit effect in a more transparent way. These parameters obey a rigorous selection rule at scattering angles of $\theta=0°$ and 180°, allowing a clear distinction to be made between the LS- and spin-orbit-coupled cases. We report numerical results in the case of the excitation of the $4s[\frac{3}{2}]_1^0$ and $4s'[\frac{1}{2}]_1^0$ levels of argon using the first-order many-body theory (FOMBT) of Csanak *et al.*,[58] with the inclusion of the spin-orbit interaction in the target states. This theory has recently been applied to the calculation of the differential cross sections (DCS) for the lowest four excited states of Ar.[59] The FOMBT is a form of the distorted-wave approximation (DWA) in which the distortion potential for both the incident and scattered electrons is the static-exchange field of the ground state. First-order many-body theory results for the 2^1P level of helium and the $3s[\frac{3}{2}]_1^0$ and the $3s'[\frac{1}{2}]_1^0$ levels of neon have been reported by Meneses *et al.*[60] and Machado *et al.*,[61] respectively. Balashov *et al.*[62] have published results of a distorted-wave calculation but in an LS-coupling scheme. Our present results are compared to the experimental data of Malcolm and McConkey[33] and Pochat *et al.*[34]

The plan of this paper is the following: in Sec. II we define the fundamental concepts to be used in interpreting the electron-photon coincidence experiments; in Sec. III we discuss the new parameters for the spin-orbit-coupled case, the simplifications for the LS-coupled case, and the selection rule which allows us to distinguish between LS- and spin-orbit-coupled systems; in Sec. IV we give a short description of our calculation for argon; and in Sec. V we present the numerical results obtained for argon, a comparison with experimental results and other theories, and our conclusions.

II. THE INTERPRETATION OF EPCE: THE FANO-MACEK FORMALISM

A. The coincidence rate for an arbitrary state of polarization: The Fano-Macek source parameters

In this section we review the fundamental formulas and concepts to be used in interpreting EPCE. In EPCE the electron-photon coincidence rate measured is proportional to the square of the dipole matrix elements averaged over the ensemble created by the collision:

$$I \propto \sum_{m_f} \langle \, | (f \,|\hat{\epsilon}^{*}\cdot\vec{r}\,|\, i) |^2 \rangle \, , \tag{1}$$

where $\sum_{m_f}$ indicates summation over all the values of the final-state magnetic quantum numbers m_f, $\langle\ \rangle$ indicates averaging over the initial m_i, $\hat{\epsilon}$ is the emitted light polarization vector, and $\vec{r}$ is the transition dipole operator of the atom.

Fano and Macek[52] take advantage of the simplicity of the definition of the polarization vector in the *detector frame* and obtain simple forms for the description of the state of polarization and for the coincidence rate using $\hat{\epsilon}^{*}\cdot\vec{r}$ in this frame. The detector frame has coordinate axes denoted by ξ, η, and ζ. ζ lies along the direction of the emitted radiation, ξ and η along the major and minor axes of the polarization ellipse, respectively. In this frame the unit polarization vector is given as

$$\hat{\epsilon} \equiv (\cos\beta, i\sin\beta, 0) \, , \tag{2}$$

where $\beta=0$ corresponds to linear polarization and $\beta=\pm\pi/4$ to right and left circular polarization.

In a next step, Fano and Macek[52] write the $\vec{r}$-dependent terms as a function of averages of first- and second-order tensors constructed with the total angular-momentum operator $\vec{J}=(J_\xi,J_\eta,J_\zeta)$. These averages are then transformed to the *collision frame* which has the z axis along the direction of the momentum of the incident electron and the $[xz]$ plane defined by the momenta of the incident and scattered electron. The notation $\vec{J}=(J_x,J_y,J_z)$ and the superscript col indicate quantities defined in this frame.

For an LS-coupled system (e.g., helium), $\vec{J}$ refers to the total *orbital* angular momentum. For a system like argon $\vec{J}$ refers to the total *electronic* angular momentum. For both spin-orbit- and LS-coupled systems, the eigenvalues of J^2 and J_z are good quantum numbers.

The resulting formula for the coincidence rate can be written (Fano and Macek[52] corrected by Briggs *et al.*[63])

$$\begin{aligned} I(\theta,\phi,\psi;\beta) = \tfrac{1}{3} CS \Bigg\{ & 1 - \frac{h^{(2)}(j_i,j_f)}{2}\left[A_0^{\text{col}}\tfrac{1}{2}(3\cos^2\theta-1) + A_{1+}^{\text{col}}\tfrac{3}{2}\sin2\theta\cos\phi + A_{2+}^{\text{col}}\tfrac{3}{2}\sin^2\theta\cos2\phi\right] \\ & + \tfrac{3}{2}h^{(2)}(j_i,j_f)\{A_0^{\text{col}}\tfrac{1}{2}\sin^2\theta\cos2\psi + A_{1+}^{\text{col}}(\sin\theta\sin\phi\sin2\psi + \sin\theta\cos\theta\cos\phi\cos2\psi) \\ & \quad + A_{2+}^{\text{col}}[\tfrac{1}{2}(1+\cos^2\theta)\cos2\psi\cos2\phi - \cos\theta\sin2\phi\sin2\psi]\}\cos2\beta \\ & + \tfrac{3}{2}h^{(1)}(j_i,j_f)O_{1-}^{\text{col}}\sin\theta\sin\phi\sin2\beta \Bigg\} \, , \end{aligned} \tag{3}$$

where θ and ϕ are the polar coordinates of the photon detector, and ψ denotes the angle between the positive ξ axis and the direction of the linear polarization. C and S are constants defined by the formulas

$$C = e^2 w_{f_i}^4 / 2\pi c^3 R^3 \, , \tag{4}$$

with w_{f_i} the frequency of the emitted radiation, c the speed of light, and R the detector's distance from the source atom, and

$$S = \frac{|\langle j_f || r || j_i \rangle|^2}{(2j_i+1)^{1/2}} \sigma(\theta_{\text{el}}) \, . \tag{5}$$

In Eq. (5) $\langle j_f \| r \| j_i \rangle$ is the reduced dipole matrix element between states $|j_f,m_f\rangle$ and $|j_i,m_i\rangle$, and $\sigma(\theta_{\rm el})$ is the electron-impact differential cross section for the excitation of the j_i level with scattered electron angle $\theta_{\rm el}$.

In Eq. (2) $h^{(1)}(j_i,j_f)$ and $h^{(2)}(j_i,j_f)$ are defined by the formula

$$h^{(k)}(j_i,j_f)=(-1)^{j_i-j_f}\frac{\begin{Bmatrix} j_i & j_i & k \\ 1 & 1 & j_f \end{Bmatrix}}{\begin{Bmatrix} j_i & j_i & k \\ 1 & 1 & j_i \end{Bmatrix}}\ , \tag{6}$$

and $A_0^{\rm col}$, $A_{1+}^{\rm col}$, $A_{2+}^{\rm col}$, and $O_{1-}^{\rm col}$ refer to the *Fano-Macek source parameters*, which are components of the alignment tensor ($A_0^{\rm col}$,$A_{1+}^{\rm col}$,$A_{2+}^{\rm col}$) and orientation vector ($O_{1-}^{\rm col}$) respectively. These parameters are defined by the formulas

$$A_0^{\rm col}=\frac{\langle 3J_z^2-J^2\rangle}{j_i(j_i+1)\sigma(\theta_{\rm el})}\ , \tag{7a}$$

$$A_{1+}^{\rm col}=\frac{\langle J_xJ_z+J_zJ_x\rangle}{j_i(j_i+1)\sigma(\theta_{\rm el})}\ , \tag{7b}$$

$$A_{2+}^{\rm col}=\frac{\langle J_x^2-J_y^2\rangle}{j_i(j_i+1)\sigma(\theta_{\rm el})}\ , \tag{7c}$$

and

$$O_{1-}^{\rm col}=\frac{\langle J_y\rangle}{j_i(j_i+1)\sigma(\theta_{\rm el})}\ , \tag{7d}$$

where the $\langle \cdots \rangle$ denotes the average

$$\langle A\rangle=\tfrac{1}{2}\sum_{m_s,m_s'}\sum_{m_i,m_i'} a^*_{m_sm_s'}(m_i')a_{m_sm_s'}(m_i)\times\langle j_i,m_i' \,|\, A \,|\, j_i,m_i\rangle\ . \tag{8}$$

The quantities $a_{m_sm_s'}(m_i)$ denote the electron-impact scattering amplitude for the excitation of the $|j_i,m_i\rangle$ sublevel with incident electron spin m_s and outgoing electron spin m_s'. We shall consider only the special case of $j_i=1$, which for LS-coupled systems includes the $n\,^1P$ levels and for spin-orbit-coupled systems (e.g., argon, neon) and the $n\,^1P_1$ and $n\,^3P_1$ levels. Substituting $j_i=1$ into Eqs. (7), we obtain the following expressions for the source parameters in terms of the scattering amplitudes:

$$A_0^{\rm col}=\frac{\langle a(1)a(1)\rangle-\langle a(0)a(0)\rangle}{\sigma_0+2\sigma_1}\ , \tag{9a}$$

$$A_{+1}^{\rm col}=\sqrt{2}\frac{{\rm Re}\langle a(0)a(1)\rangle}{\sigma_0+2\sigma_1}\ , \tag{9b}$$

$$A_{2+}^{\rm col}=\frac{\langle a(-1)a(1)\rangle}{\sigma_0+2\sigma_1}\ , \tag{9c}$$

and

$$O_{1-}^{\rm col}=-\sqrt{2}\frac{{\rm Im}\langle a(0)a(1)\rangle}{\sigma_0+2\sigma_1}\ , \tag{9d}$$

where

$$\langle a(m')a(m)\rangle=\tfrac{1}{2}\sum_{m_s,m_s'} a^*_{m_sm_s'}(m')a_{m_sm_s'}(m)\ , \tag{10}$$

and

$$\sigma_m=\langle a(m)a(m)\rangle \tag{11}$$

refers to the DCS for the excitation of the $|j,m\rangle$ sublevel of the j level.[64] In deriving Eqs. (9) the following symmetry relation was used:

$$\langle a(m')a(m)\rangle=(-1)^{m+m'}\langle a(-m')a(-m)\rangle\ . \tag{12}$$

B. The Stokes parameters

The expression given by Eq. (3) gives the intensity of emitted radiation into the (θ,ϕ) direction with polarization parameters (ψ,β), where ψ is the angle "of linear polarization" and β is the "phase parameter" as discussed earlier. The emitted radiation can also be characterized by the Stokes parameters, an appproach used by Blum and Kleinpoppen.[53]

The Stokes parameters I, I_{η_1}, I_{η_2}, and I_{η_3} are defined by the following equations:

$$I(\theta,\phi)=I(\theta,\phi,0;0)+I(\theta,\phi,\tfrac{1}{2}\pi;0)\ , \tag{13a}$$

$$I_{\eta_1}(\theta,\phi)=I(\theta,\phi,\tfrac{1}{4}\pi;0)-I(\theta,\phi,\tfrac{3}{4}\pi;0)\ , \tag{13b}$$

$$I_{\eta_2}(\theta,\phi)=I(\theta,\phi,\psi;\tfrac{1}{4}\pi)-I(\theta,\phi,\psi;-\tfrac{1}{4}\pi)\ , \tag{13c}$$

and

$$I_{\eta_3}(\theta,\phi)=I(\theta,\phi,0;0)-I(\theta,\phi,\tfrac{1}{2}\pi;0)\ . \tag{13d}$$

$I(\theta,\phi)$ can be interpreted as the polarization averaged coincidence rate measured in the angular-correlation experiment. From Eqs. (3) and (13a) we have

$$I(\theta,\phi)=\tfrac{2}{3}CS\left[1-\frac{h^{(2)}(j_i,j_f)}{2}[A_0^{\rm col}\tfrac{1}{2}(3\cos^2\theta-1)+A_{1+}^{\rm col}\tfrac{3}{2}\sin 2\theta\cos\phi+A_{2+}^{\rm col}\tfrac{3}{2}\sin^2\theta\cos 2\phi]\right]\ . \tag{14}$$

This formula clearly shows that from an angular-correlation experiment, where $I(\theta,\phi)$ is measured for a series of values of θ and ϕ, the $A_0^{\rm col}$, $A_1^{\rm col}$, and $A_{2+}^{\rm col}$ parameters can be extracted, but not $O_{1-}^{\rm col}$.

The quantities η_1, η_2, and η_3 appearing in Eqs. (13b)–(13d) can be interpreted as the degree of linear polarization at angle $\pi/4$ relative to the ξ axis, the degree of circular polarization, and the degree of linear polarization along the ξ axis, respectively. In a polarization-correlation experiment the intensities I, I_{η_1}, I_{η_2}, and I_{η_3} are measured in arbitrary units; in effect, this experiment can be considered as a measurement of η_1, η_2, and η_3.

From Eqs. (13b)–(13d) and (3) one can obtain the appropriate formulas for η_1, η_2, and η_3 for the angles $\theta=\pi/2$ and $\phi=\pi/2$, commonly used in these experiments:

$$\eta_1 \equiv I_{\eta_1}(\tfrac{1}{2}\pi,\tfrac{1}{2}\pi) = \frac{6A^{\rm col}_{1+}}{4+A^{\rm col}_{0+}+3A^{\rm col}_{2+}} , \tag{15a}$$

$$\eta_2 \equiv I_{\eta_2}(\tfrac{1}{2}\pi,\tfrac{1}{2}\pi) = -\frac{6O^{\rm col}_{1-}}{4+A^{\rm col}_{0+}+3A^{\rm col}_{2+}} , \tag{15b}$$

and

$$\eta_3 \equiv I_{\eta_3}(\tfrac{1}{2}\pi,\tfrac{1}{2}\pi) = \frac{3(A^{\rm col}_{2+}-A^{\rm col}_{0})}{4+A^{\rm col}_{0}+3A^{\rm col}_{2+}} . \tag{15c}$$

These formulas show that the measurement of η_1, η_2, and η_3 in the polarization-correlation experiment will give information about the Fano-Macek source parameters, but a single measurement of η_1, η_2, and η_3 will not allow a determination of all four source parameters. If all source parameters are not independent (e.g., in the *LS*-coupled case), then a single polarization-correlation experiment is sufficient to obtain complete information. In the general case (e.g., spin-orbit-coupled systems) angular- and polarization-correlation experiments have to be combined to determine all Fano-Macek source parameters or any equivalent set of coherence and correlation parameters.

Finally, we note that sometimes it is convenient to use quantities related to η_1, η_2, and η_3. Born and Wolf[65] defined the degree of polarization, P, and the correlation factor μ by the formulas

$$P = (\eta_1^2+\eta_2^2+\eta_3^2)^{1/2} , \tag{16}$$

and

$$\mu = |\mu| e^{i\delta} = \frac{\eta_1+i\eta_2}{(1-\eta_3^2)^{1/2}} . \tag{17}$$

Evidently the measurement of η_1, η_2, and η_3 is equivalent to the measurement of P and μ. The radiation field is polarized and coherent if

$$P=1 . \tag{18}$$

III. COHERENCE AND CORRELATION PARAMETERS

A. *LS*-coupled case

The first EPCE measurements were made for the $n\,^1P$ ($n=2,3$) excitation of helium. Blum and Kleinpoppen[53] showed that the Fano-Macek source parameters in the case of *LS*-coupling can be expressed in terms of the λ and χ parameters of Eminyan *et al.*[15] This implies that in the *LS*-coupled case not all the Fano-Macek source parameters are independent. This fact is the consequence of the factorization of the spin-dependent part and of mirror symmetry of the scattering amplitude. These can be expressed by the following relations: Factorizing the spin gives

$$a_{m_s m_s'}(m_i) = a_{m_s}\delta_{m_s m_s'} , \tag{19}$$

and the plane symmetry is expressed by the relation

$$a_{-m} = (-1)^m a_m . \tag{20}$$

By substituting Eqs. (19) and (20) into Eqs. (9), we can show that only two source parameters are independent and that all source parameters can be expressed in terms of the λ and χ parameters defined by the equations

$$\lambda = \frac{\sigma_0}{\sigma_0+\sigma_1} , \tag{21}$$

where

$$\sigma_m = |a_m|^2 \quad (m=0,\pm 1) ,$$

and

$$\chi = \arg(a_1) - \arg(a_0) . \tag{22}$$

The expressions for the source parameters are

$$A^{\rm col}_0 = \tfrac{1}{2}(1-3\lambda) , \tag{23a}$$

$$A^{\rm col}_{1+} = [\lambda(1-\lambda)]^{1/2}\cos\chi , \tag{23b}$$

$$A^{\rm col}_{2+} = \tfrac{1}{2}(\lambda-1) , \tag{23c}$$

and

$$O^{\rm col}_{1-} = -[\lambda(1-\lambda)^{1/2}]\sin\chi . \tag{23d}$$

As discussed earlier the angular-correlation experiment measures the alignment parameters ($A^{\rm col}_{0+}, A^{\rm col}_{1+}, A^{\rm col}_{2+}$). From Eqs. (23) we observe that the angular-correlation experiment allows the determination of λ and $\cos\chi$, or equivalently λ and $|\chi|$. From Eqs. (23) and (15) we obtain

$$\eta_i = 2[\lambda(1-\lambda)]^{1/2}\cos\chi , \tag{24a}$$

$$\eta_2 = -2[\lambda(1-\lambda)]^{1/2}\sin\chi , \tag{24b}$$

and

$$\eta_3 = 2\lambda - 1 . \tag{24c}$$

Since the polarization-correlation experiments determine the η_1, η_2, and η_3 parameters, it follows from Eqs. (24) that these experiments determine λ, $\cos\chi$, and $\sin\chi$, or equivalently λ and χ. From Eqs. (16) and (24) it follows that, for *LS* coupling, $P=1$, signifying that the ensemble excited by the electron is in a coherent state. This is a consequence of the fact that the coherence properties of the emitted radiation are not affected by an electron beam in an unpolarized spin state since there is no spin-orbit-coupling effect present and the "spin incoherence" does not transfer to the photon field.

B. Spin-orbit-coupled case

If the spin-orbit interaction has to be included in the electron scattering process (i.e., if the spin-orbit-coupling effect is important either for the scattering or for the target electrons) the four Fano-Macek source parameters remain independent. It is interesting to see whether the λ and χ parameters, used for *LS*-coupled systems, can be generalized and extended for this case. Such parametrization was introduced by da Paixão *et al.*[57] An alternative view was suggested by Hermann and Hertel.[66]

The parameters suggested by da Paixão *et al.* for the case where the spin-orbit coupling is present in the target state are defined by the formulas

$$\lambda=\frac{\sigma_0}{\sigma_0+2\sigma_1}\ , \qquad (25a)$$

$$\cos\Delta=\frac{|\langle a(0)a(1)\rangle|}{\sqrt{\sigma_0\sigma_1}}\ , \qquad (25b)$$

$$\cos\bar{\chi}=\frac{\mathrm{Re}\langle a(0)a(1)\rangle}{|\langle a(0)a(1)\rangle|}\ , \qquad (25c)$$

and

$$\cos\epsilon=-\frac{\langle a(1)a(-1)\rangle}{\sigma_1}\ . \qquad (25d)$$

The equivalent Fano-Macek source parameters can be given in terms of these new parameters by the following relations:

$$A_0^{\mathrm{col}}=\tfrac{1}{2}(1-3\lambda)\ , \qquad (26a)$$

$$A_{1+}^{\mathrm{col}}=[\lambda(1-\lambda)]^{1/2}\cos\bar{\chi}\cos\Delta\ , \qquad (26b)$$

$$A_{2+}^{\mathrm{col}}=\tfrac{1}{2}(\lambda-1)\cos\epsilon\ , \qquad (26c)$$

and

$$O_{1-}^{\mathrm{col}}=-[\lambda(1-\lambda)]^{1/2}\sin\bar{\chi}\cos\Delta\ . \qquad (26d)$$

From these formulas we obtain for the η_1,η_2,η_3 parameters

$$\eta_1=\frac{4[\lambda(1-\lambda)]^{1/2}\cos\bar{\chi}\cos\Delta}{(3-\cos\epsilon)+(\cos\epsilon-1)\lambda}\ , \qquad (27a)$$

$$\eta_2=\frac{-4[\lambda(1-\lambda)]^{1/2}\sin\bar{\chi}\cos\Delta}{(3-\cos\epsilon)+(\cos\epsilon-1)\lambda}\ , \qquad (27b)$$

and

$$\eta_3=\frac{(1+\cos\epsilon)-(3+\cos\epsilon)\lambda}{(3-\cos\epsilon)+(\cos\epsilon-1)\lambda}\ , \qquad (27c)$$

For P and μ we have [see Eq. (17)]

$$P=\left[1-\frac{8[1-\cos\epsilon+2\lambda(\cos\epsilon-\cos^2\Delta)+\lambda^2(2\cos^2\Delta-\cos\epsilon-1)]}{3-\cos\epsilon+\lambda(\cos\epsilon-1)]^2}\right]^{1/2}\ , \qquad (28a)$$

$$|\mu|=\frac{\sqrt{2\lambda}\cos\Delta}{[1-\cos\epsilon+\lambda(1+\cos\epsilon)]^{1/2}}\ , \qquad (28b)$$

and

$$\delta=-\bar{\chi}\ . \qquad (28c)$$

Setting the spin-orbit interaction to zero, we recover the LS-coupled case. The λ parameter remains the same, and $\bar{\chi}$ goes to χ. Using the spin factorization given by Eq. (19) and the plane symmetry given by Eq. (20), we obtain from Eqs. (25b) and (25d), in the LS coupling limit,

$$\cos\Delta\equiv 1 \qquad (29a)$$

and

$$\cos\epsilon\equiv 1 \qquad (29b)$$

for all angles where $\sigma_0\neq 0,\sigma_1\neq 0$ and $\sigma_1\neq 0$, respectively.

for all angles where $\sigma_0\neq 0$, and $\sigma_1\neq 0$, respectively. Since at $\theta_{\mathrm{el}}=0°$ and 180° in the LS-coupling case $\sigma_1=0$, we can define the value of $\cos\Delta$ and $\cos\epsilon$ at $\theta_{\mathrm{el}}=0°$ and 180° as a limit and state that the identities (29) hold for arbitrary angles (including $\theta_{\mathrm{el}}=0°$ and 180°).

C. Selection rule

One of the advantages of the parameters λ, $\bar{\chi}$, ϵ, and Δ defined by Eqs. (25) is that they show the spin-orbit coupling in a very transparent way. A selection rule requires that the parameters ϵ and Δ go to $\pi/2$ at $\theta_l=0°$ and 180° in the presence of spin-orbit coupling, while their limit in the LS-coupled case is zero. As we mentioned before, if LS coupling holds, ϵ and Δ are zero for all angles.

To prove that $\cos\Delta=0$ and $\cos\epsilon=0$ at $\theta_{\mathrm{el}}=0°$ and 180°

TABLE I. λ parameter for the excitation of the $4s[\frac{3}{2}]_1^0({}^3P_1)$ state of argon.

Angle (deg)	16.0 eV	20.0 eV	30.0 eV	50.0 eV	80.4 eV
0	0.992	0.957	0.975	1.000	1.000
5	0.971	0.916	0.838	0.701	0.449
10	0.911	0.806	0.546	0.328	0.134
15	0.813	0.651	0.276	0.102	0.056
20	0.684	0.481	0.128	0.024	0.308
25	0.537	0.331	0.171	0.365	0.851
30	0.401	0.249	0.366	0.813	0.983
35	0.319	0.270	0.565	0.899	0.958
40	0.315	0.370	0.684	0.881	0.935
45	0.364	0.483	0.733	0.853	0.923
50	0.422	0.566	0.739	0.825	0.907
55	0.465	0.612	0.717	0.787	0.869
60	0.487	0.629	0.673	0.717	0.781

TABLE I. (*Continued*).

Angle (deg)	16.0 eV	20.0 eV	30.0 eV	50.0 eV	80.4 eV
65	0.488	0.623	0.615	0.561	0.660
70	0.475	0.564	0.548	0.298	0.587
75	0.450	0.565	0.482	0.186	0.561
80	0.417	0.519	0.420	0.272	0.557
85	0.382	0.462	0.364	0.357	0.569
90	0.349	0.400	0.313	0.408	0.591
95	0.323	0.337	0.264	0.437	0.620
100	0.309	0.285	0.221	0.460	0.658
105	0.308	0.254	0.190	0.483	0.706
110	0.321	0.247	0.180	0.512	0.765
115	0.341	0.260	0.200	0.546	0.829
120	0.365	0.283	0.245	0.559	0.868
125	0.389	0.307	0.300	0.504	0.807
130	0.411	0.328	0.351	0.389	0.559
135	0.428	0.349	0.391	0.308	0.270
140	0.442	0.355	0.418	0.293	0.231
145	0.452	0.362	0.436	0.322	0.365
150	0.459	0.366	0.447	0.378	0.518
155	0.463	0.368	0.453	0.449	0.653
160	0.466	0.368	0.456	0.529	0.767
165	0.467	0.368	0.458	0.608	0.855
170	0.467	0.367	0.460	0.676	0.912
175	0.467	0.367	0.462	0.721	0.941
180	0.467	0.367	0.462	0.737	0.950

TABLE II. $\bar{\chi}$ parameter for the excitation of the $4s[\frac{3}{2}]_1^0(^3P_1)$ state of argon.

Angle (deg)	16.0 eV	20.0 eV	30.0 eV	50.0 eV	80.4 eV
0	0.000	0.000	0.000	0.000	0.000
5	0.037	0.085	0.154	0.017	0.102
10	0.050	0.093	0.225	0.036	0.353
15	0.076	0.106	0.398	0.108	1.378
20	0.128	0.121	0.848	2.048	2.407
25	0.231	0.131	1.725	2.693	2.624
30	0.443	0.108	2.222	2.276	0.955
35	0.846	0.132	2.261	1.447	0.160
40	1.324	1.589	1.807	1.004	0.243
45	1.588	2.003	0.999	0.826	0.415
50	1.631	1.891	0.701	0.703	0.684
55	1.529	1.624	0.679	0.546	1.099
60	1.330	1.267	0.777	0.308	1.668
65	1.082	0.891	0.996	0.010	2.302
70	0.836	0.630	1.239	0.388	2.853
75	0.627	0.335	1.548	1.904	3.008
80	0.463	0.174	1.805	2.954	2.683
85	0.337	0.070	1.963	2.782	2.428
90	0.238	0.007	2.025	2.718	2.221
95	0.155	0.026	2.009	2.691	2.042
100	0.079	0.038	1.936	2.686	1.881

TABLE II. (*Continued*).

Angle (deg)	16.0 eV	20.0 eV	30.0 eV	50.0 eV	80.4 eV
105	0.004	0.030	1.837	2.701	1.737
110	0.115	0.001	1.783	2.754	1.607
115	0.307	0.076	1.928	2.911	1.475
120	0.742	0.625	2.527	2.704	1.200
125	1.616	2.853	3.137	1.117	0.491
130	2.225	3.006	2.900	0.547	0.950
135	2.469	3.074	2.816	0.095	0.494
140	2.581	3.100	2.784	0.331	0.288
145	2.640	3.128	2.772	0.629	0.627
150	2.675	3.132	2.770	0.798	0.741
155	2.696	3.110	2.772	0.886	0.791
160	2.709	3.096	2.776	0.929	0.825
165	2.717	3.084	2.780	0.947	0.857
170	2.721	3.075	2.783	0.954	0.891
175	2.724	3.069	2.785	0.955	0.919
180	0.000	0.000	0.000	0.000	0.000

TABLE III. χ parameter for the excitation of the $4s[\frac{3}{2}]_1^0(^3P_1)$ state of argon.

Angle (deg)	16.0 eV	20.0 eV	30.0 eV	50.0 eV	80.4 eV
0	1.571	1.571	1.571	1.571	1.571
5	0.657	0.827	0.447	0.036	0.105
10	0.489	0.544	0.353	0.078	0.363
15	0.485	0.456	0.474	0.247	1.384
20	0.549	0.474	0.952	1.831	2.376
25	0.674	0.621	1.667	2.536	2.485
30	0.878	0.944	1.886	2.173	1.346
35	1.161	1.334	1.810	1.465	0.537
40	1.433	1.573	1.626	1.075	0.510
45	1.581	1.651	1.428	0.926	0.644
50	1.603	1.637	1.274	0.844	0.860
55	1.551	1.582	1.197	0.754	1.183
60	1.464	1.510	1.205	0.623	1.655
65	1.362	1.431	1.286	0.506	2.235
70	1.255	1.353	1.415	0.765	2.695
75	1.145	1.256	1.560	1.645	2.750
80	1.034	1.150	1.690	2.211	2.551
85	0.929	1.024	1.783	2.387	2.348
90	0.845	0.881	1.829	2.441	2.172
95	0.809	0.740	1.828	2.451	2.014
100	0.848	0.669	1.787	2.436	1.865
105	0.959	0.763	1.723	2.393	1.728
110	1.114	1.000	1.676	2.304	1.604
115	1.279	1.273	1.695	2.135	1.492
120	1.437	1.518	1.787	1.831	1.385
125	1.577	1.718	1.917	1.400	1.321
130	1.698	1.872	2.049	1.011	1.239
135	1.797	1.977	2.164	0.833	0.935
140	1.874	2.064	2.251	0.860	0.650
145	1.926	2.107	2.304	0.949	0.744

TABLE III. (*Continued*).

Angle (deg)	16.0 eV	20.0 eV	30.0 eV	50.0 eV	80.4 eV
150	1.953	2.116	2.316	1.027	0.822
155	1.951	2.088	2.283	1.087	0.875
160	1.920	2.032	2.206	1.142	0.934
165	1.862	1.945	2.089	1.206	1.021
170	1.780	1.835	1.937	1.296	1.154
175	1.680	1.707	1.760	1.420	1.343
180	1.571	1.571	1.571	1.571	1.571

TABLE IV. Δ parameter for the excitation of the $4s[\frac{3}{2}]_1^0(^3P_1)$ state of argon.

Angle (deg)	16.0 eV	20.0 eV	30.0 eV	50.0 eV	80.4 eV
0	1.571	1.571	1.571	1.571	1.571
5	0.656	0.824	0.421	0.032	0.026
10	0.487	0.537	0.274	0.069	0.084
15	0.480	0.445	0.264	0.223	0.260
20	0.535	0.460	0.502	0.977	0.238
25	0.639	0.608	0.891	0.422	0.423
30	0.785	0.940	1.033	0.509	1.174
35	0.926	1.332	1.189	0.548	0.515
40	0.973	1.453	1.331	0.479	0.452
45	0.980	1.379	1.304	0.479	0.507
50	1.015	1.357	1.178	0.515	0.570
55	1.067	1.362	1.082	0.550	0.587
60	1.106	1.365	1.045	0.550	0.518
65	1.115	1.348	1.053	0.506	0.393
70	1.089	1.300	1.072	0.677	0.346
75	1.035	1.237	1.068	1.343	0.369
80	0.962	1.143	1.034	0.917	0.386
85	0.883	1.023	0.987	0.678	0.383
90	0.819	0.881	0.949	0.576	0.364
95	0.797	0.740	0.927	0.543	0.337
100	0.845	0.668	0.924	0.559	0.318
105	0.959	0.762	0.955	0.627	0.330
110	1.110	1.000	1.053	0.762	0.408
115	1.264	1.272	1.210	0.989	0.610
120	1.388	1.506	1.305	1.283	1.034
125	1.423	1.418	1.224	1.173	1.287
130	1.361	1.267	1.077	0.900	0.976
135	1.280	1.163	0.939	0.829	0.830
140	1.211	1.077	0.834	0.809	0.591
145	1.163	1.034	0.771	0.767	0.431
150	1.140	1.026	0.757	0.737	0.395
155	1.147	1.054	0.794	0.745	0.423
160	1.184	1.109	0.882	0.802	0.503
165	1.250	1.196	1.013	0.914	0.646
170	1.342	1.306	1.179	1.084	0.872
175	1.451	1.434	1.368	1.309	1.189
180	1.571	1.571	1.571	1.571	1.571

TABLE V. ϵ parameter for the excitation of the $4s[\frac{3}{2}]_1^0(^3P_1)$ state of argon.

Angle (deg)	16.0 eV	20.0 eV	30.0 eV	50.0 eV	80.4 eV
0	1.571	1.571	1.571	1.571	1.571
5	1.025	1.144	0.621	0.046	0.033
10	0.883	0.867	0.475	0.076	0.071
15	0.901	0.812	0.523	0.142	0.151
20	0.978	0.867	0.666	0.260	0.311
25	1.095	0.994	0.894	0.484	0.745
30	1.243	1.180	1.209	0.885	2.023
35	1.414	1.417	1.591	1.028	0.940
40	1.593	1.691	1.955	0.858	0.780
45	1.753	1.968	2.152	0.797	0.821
50	1.868	2.189	2.104	0.817	0.881
55	1.919	2.279	1.915	0.874	0.878
60	1.908	2.223	1.701	0.943	0.797
65	1.858	2.081	1.508	0.995	0.696
70	1.790	1.916	1.351	1.001	0.609
75	1.722	1.759	1.234	0.971	0.542
80	1.665	1.620	1.154	0.941	0.496
85	1.623	1.503	1.105	0.926	0.472
90	1.599	1.410	1.082	0.927	0.467
95	1.592	1.345	1.075	0.945	0.480
100	1.601	1.309	1.081	0.983	0.523
105	1.622	1.302	1.095	1.050	0.619
110	1.651	1.319	1.115	1.161	0.801
115	1.681	1.352	1.135	1.324	1.134
120	1.709	1.391	1.155	1.482	1.643
125	1.731	1.429	1.173	1.435	1.629
130	1.742	1.463	1.194	1.201	1.152
135	1.744	1.512	1.220	1.019	0.853
140	1.735	1.511	1.253	0.939	0.684
145	1.718	1.527	1.294	0.925	0.604
150	1.694	1.540	1.340	0.953	0.588
155	1.667	1.551	1.391	1.013	0.630
160	1.638	1.557	1.442	1.103	0.731
165	1.612	1.563	1.491	1.226	0.904
170	1.590	1.567	1.532	1.374	1.156
175	1.576	1.570	1.561	1.511	1.435
180	1.571	1.571	1.571	1.571	1.571

TABLE VI. λ parameter for the excitation of the $4s'[\frac{1}{2}]_1^0(^1P_1)$ state of argon.

Angle (deg)	16.0 eV	20.0 eV	30.0 eV	50.0 eV	80.4 eV
0	0.999	0.997	0.998	1.000	1.000
5	0.982	0.958	0.862	0.701	0.449
10	0.929	0.852	0.569	0.328	0.134
15	0.843	0.699	0.287	0.099	0.053
20	0.726	0.517	0.107	0.009	0.305
25	0.575	0.317	0.128	0.356	0.868
30	0.397	0.127	0.399	0.837	0.997

TABLE VI. (*Continued*).

Angle (deg)	16.0 eV	20.0 eV	30.0 eV	50.0 eV	80.4 eV
35	0.231	0.045	0.721	0.925	0.968
40	0.196	0.220	0.898	0.906	0.946
45	0.383	0.553	0.946	0.883	0.937
50	0.639	0.796	0.928	0.865	0.926
55	0.805	0.906	0.874	0.841	0.894
60	0.877	0.941	0.799	0.787	0.812
65	0.891	0.938	0.714	0.633	0.696
70	0.873	0.897	0.631	0.270	0.623
75	0.831	0.874	0.564	0.064	0.593
80	0.767	0.818	0.514	0.206	0.584
85	0.682	0.740	0.476	0.341	0.590
90	0.574	0.637	0.441	0.423	0.607
95	0.447	0.505	0.400	0.477	0.633
100	0.314	0.353	0.348	0.524	0.669
105	0.198	0.206	0.284	0.579	0.719
110	0.122	0.096	0.220	0.653	0.788
115	0.098	0.044	0.182	0.746	0.874
120	0.123	0.047	0.187	0.810	0.954
125	0.182	0.091	0.231	0.701	0.946
130	0.262	0.158	0.294	0.433	0.689
135	0.350	0.247	0.360	0.270	0.315
140	0.441	0.324	0.426	0.248	0.255
145	0.532	0.414	0.491	0.303	0.395
150	0.619	0.507	0.559	0.397	0.551
155	0.702	0.602	0.632	0.516	0.689
160	0.777	0.691	0.709	0.646	0.808
165	0.841	0.773	0.788	0.773	0.899
170	0.890	0.840	0.859	0.880	0.958
175	0.921	0.884	0.911	0.952	0.988
180	0.932	0.900	0.93	0.978	0.997

TABLE VII. $\bar{\chi}$ parameter for the excitation of the $4s'[\frac{1}{2}]_1^0(^1P_1)$ state of argon.

Angle (deg)	16.0 eV	20.0 eV	30.0 eV	50.0 eV	80.4 eV
0	0.000	0.000	0.000	0.000	0.000
5	0.022	0.066	0.150	0.017	0.102
10	0.030	0.069	0.219	0.036	0.352
15	0.047	0.074	0.392	0.110	1.374
20	0.079	0.076	0.909	2.048	2.417
25	0.142	0.067	2.034	2.698	2.645
30	0.280	0.003	2.538	2.302	1.002
35	0.636	1.304	2.640	1.472	0.170
40	1.427	2.770	2.460	1.007	0.261
45	2.007	2.860	1.731	0.822	0.438
50	2.155	2.922	1.105	0.700	0.702
55	2.057	3.064	0.970	0.551	1.090
60	1.675	2.422	1.016	0.319	1.627

TABLE VII. (*Continued*).

Angle (deg)	16.0 eV	20.0 eV	30.0 eV	50.0 eV	80.4 eV
65	1.031	0.855	1.142	0.020	2.274
70	0.576	0.639	1.311	0.513	2.861
75	0.367	0.485	1.496	2.139	2.991
80	0.272	0.407	1.665	3.116	2.676
85	0.226	0.336	1.801	2.898	2.434
90	0.201	0.265	1.898	2.814	2.237
95	0.179	0.194	1.963	2.782	2.062
100	0.139	0.124	2.013	2.782	1.899
105	0.046	0.059	2.078	2.817	1.746
110	0.201	0.014	2.212	2.914	1.598
115	0.830	0.084	2.468	3.120	1.425
120	1.552	2.612	2.795	2.462	1.013
125	1.863	2.749	3.047	1.487	0.547
130	1.973	2.718	3.095	0.841	0.915
135	2.010	2.637	3.024	0.298	0.546
140	2.016	2.617	2.991	0.168	0.200
145	2.007	2.567	2.979	0.468	0.578
150	1.993	2.522	2.977	0.637	0.708
155	1.977	2.475	2.980	0.721	0.763
160	1.961	2.447	2.985	0.767	0.797
165	1.948	2.420	2.989	0.790	0.831
170	1.938	2.400	2.992	0.800	0.866
175	1.932	2.388	2.994	0.804	0.895
180	0.000	0.000	0.000	0.000	0.000

TABLE VIII. χ parameter for the excitation of the $4s'[\frac{1}{2}]_1^0(^1P_1)$ state of argon.

Angle (deg)	16.0 eV	20.0 eV	30.0 eV	50.0 eV	80.4 eV
0	1.571	1.571	1.571	1.571	1.571
5	0.198	0.282	0.188	0.019	0.102
10	0.139	0.170	0.231	0.040	0.352
15	0.141	0.145	0.397	0.124	1.375
20	0.170	0.150	0.917	2.017	2.415
25	0.234	0.194	2.013	2.685	2.633
30	0.375	0.394	2.465	2.294	1.104
35	0.724	1.494	2.497	1.473	0.223
40	1.443	2.370	2.253	1.013	0.288
45	1.958	2.485	1.683	0.831	0.458
50	2.058	2.403	1.192	0.713	0.717
55	1.924	2.151	1.034	0.571	1.097
60	1.632	1.734	1.056	0.357	1.627
65	1.280	1.316	1.167	0.152	2.269
70	0.983	1.050	1.325	0.551	2.846
75	0.770	0.829	1.499	2.044	2.962
80	0.621	0.684	1.661	2.852	2.666
85	0.514	0.560	1.791	2.829	2.428
90	0.436	0.447	1.884	2.776	2.233
95	0.388	0.342	1.946	2.750	2.060
100	0.387	0.267	1.994	2.747	1.898

TABLE VIII. (*Continued*).

Angle (deg)	16.0 eV	20.0 eV	30.0 eV	50.0 eV	80.4 eV
105	0.483	0.293	2.053	2.756	1.745
110	0.745	0.524	2.168	2.805	1.598
115	1.170	1.090	2.370	2.783	1.428
120	1.559	1.858	2.592	2.321	1.065
125	1.788	2.273	2.729	1.494	0.750
130	1.899	2.430	2.791	0.877	0.949
135	1.947	2.452	2.820	0.392	0.589
140	1.961	2.474	1.836	0.298	0.257
145	1.957	2.445	2.842	0.516	0.589
150	1.942	2.402	2.833	0.664	0.715
155	1.920	2.343	2.801	0.749	0.769
160	1.891	2.281	2.736	0.799	0.807
165	1.852	2.191	2.622	0.836	0.847
170	1.794	2.058	2.426	0.889	0.902
175	1.701	1.852	2.087	1.039	1.014
180	1.571	1.571	1.571	1.571	1.571

TABLE IX. Δ parameter for the excitation of the $4s'[\frac{1}{2}]_1^0(^1P_1)$ state of argon.

Angle (deg)	16.0 eV	20.0 eV	30.0 eV	50.0 eV	80.4 eV
0	1.571	1.571	1.571	1.571	1.571
5	0.196	0.274	0.114	0.008	0.007
10	0.136	0.155	0.072	0.018	0.021
15	0.133	0.125	0.070	0.057	0.068
20	0.151	0.130	0.149	0.352	0.062
25	0.187	0.182	0.294	0.111	0.113
30	0.252	0.394	0.328	0.138	0.583
35	0.372	1.274	0.423	0.157	0.145
40	0.475	0.693	0.624	0.135	0.123
45	0.467	0.601	0.793	0.135	0.139
50	0.555	0.711	0.604	0.147	0.157
55	0.736	0.988	0.440	0.160	0.161
60	0.936	1.353	0.366	0.163	0.141
65	0.980	1.176	0.338	0.150	0.107
70	0.848	0.902	0.329	0.210	0.094
75	0.693	0.702	0.322	0.563	0.098
80	0.566	0.566	0.312	0.288	0.102
85	0.465	0.457	0.301	0.198	0.100
90	0.389	0.364	0.292	0.166	0.095
95	0.346	0.284	0.288	0.157	0.088
100	0.362	0.237	0.290	0.166	0.083
105	0.481	0.287	0.303	0.194	0.087
110	0.722	0.524	0.344	0.250	0.110
115	0.954	1.088	0.410	0.358	0.180
120	0.893	1.236	0.436	0.503	0.413
125	0.727	0.796	0.402	0.420	0.542
130	0.605	0.590	0.347	0.288	0.299
135	0.529	0.491	0.300	0.259	0.232
140	0.486	0.434	0.267	0.247	0.162

TABLE IX. (*Continued*).

Angle (deg)	16.0 eV	20.0 eV	30.0 eV	50.0 eV	80.4 eV
145	0.472	0.419	0.253	0.227	0.116
150	0.483	0.433	0.262	0.215	0.106
155	0.522	0.480	0.301	0.220	0.114
160	0.595	0.558	0.376	0.249	0.139
165	0.716	0.685	0.499	0.311	0.189
170	0.906	0.883	0.703	0.440	0.294
175	1.193	1.180	1.048	0.751	0.564
180	1.571	1.571	1.571	1.571	1.571

TABLE X. ϵ parameter for the excitation of the $4s'[\frac{1}{2}]_1^0(^1P_1)$ state of argon.

Angle (deg)	16.0 eV	20.0 eV	30.0 eV	50.0 eV	80.4 eV
0	1.571	1.571	1.571	1.571	1.571
5	0.315	0.402	0.171	0.012	0.008
10	0.248	0.253	0.126	0.019	0.018
15	0.251	0.228	0.139	0.036	0.038
20	0.275	0.243	0.181	0.066	0.080
25	0.317	0.284	0.255	0.125	0.200
30	0.377	0.350	0.380	0.242	1.059
35	0.461	0.449	0.601	0.296	0.267
40	0.578	0.594	1.003	0.243	0.214
45	0.745	0.816	1.379	0.227	0.228
50	0.980	1.161	1.108	0.236	0.247
55	1.286	1.670	0.795	0.259	0.245
60	1.561	2.067	0.611	0.283	0.220
65	1.581	1.800	0.501	0.295	0.190
70	1.377	1.371	0.433	0.287	0.165
75	0.151	1.061	0.392	0.271	0.146
80	0.974	0.849	0.370	0.261	0.132
85	0.846	0.699	0.360	0.258	0.125
90	0.755	0.590	0.359	0.261	0.122
95	0.690	0.513	0.362	0.272	0.125
100	0.645	0.462	0.367	0.291	0.137
105	0.614	0.431	0.369	0.326	0.163
110	0.595	0.417	0.367	0.390	0.216
115	0.584	0.416	0.360	0.512	0.336
120	0.580	0.425	0.353	0.673	0.693
125	0.583	0.440	0.348	0.563	0.793
130	0.591	0.462	0.350	0.376	0.381
135	0.606	0.501	0.361	0.291	0.248
140	0.628	0.523	0.381	0.262	0.189
145	0.660	0.567	0.413	0.259	0.164
150	0.706	0.625	0.460	0.273	0.159
155	0.772	0.705	0.527	0.303	0.172
160	0.868	0.811	0.624	0.354	0.206
165	1.009	0.966	0.772	0.445	0.274
170	1.208	1.181	1.003	0.619	0.416
175	1.444	1.434	1.339	1.011	0.777
180	1.571	1.571	1.571	1.571	1.571

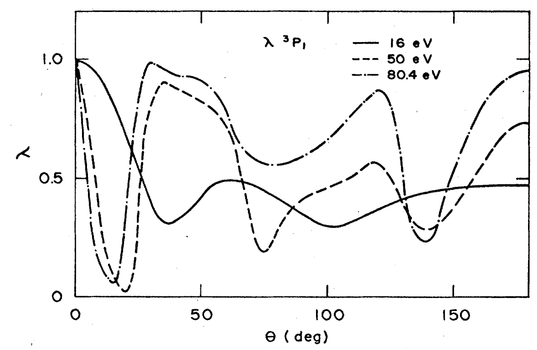

FIG. 1. λ parameter for the $4s[\frac{3}{2}]_1^0(^3P_1)$ state.

in the spin-orbit-coupled case, we must recall the definition of $\cos\Delta$ and $\cos\epsilon$ given by Eqs. (27a) and (25d), respectively. We need only to prove that at these angles $\langle a(0)a(1)\rangle=0$ and $\langle a(1)a(-1)\rangle=0$ while simultaneously $\sigma_0\neq0$ and $\sigma_1\neq0$. The proof is based on the conservation of angular momentum. If the electron is scattered into the forward ($\theta_{\rm el}=0$) or backward ($\theta_{\rm el}=180°$) direction then its *orbital* angular-momentum projection is zero. The projection of the incident electron angular momentum is also zero. Thus the angular-momentum conservation can be written as

$$m_s+m_{j_0}=m_s'+m_j\ . \tag{30}$$

If the original state is $^1S_0$ then $j_0=0$ and $m_{j_0}\equiv0$, consequently

$$m_s=m_s'+m_j\ . \tag{31}$$

By definition,

$$\langle a(0)a(1)\rangle=\sum_{m_s,m_s'}[a(0)]_{m_sm_s'}[a(1)]_{m_sm_s'}\ .$$

From (31) it is clear that the $[a(0)]_{m_sm_s'}$ amplitude is different from zero only if $m_s=m_s'$, whereas $[a(1)]_{m_sm_s'}$ is different from zero *only* if $m_s=m_s'+1$. Thus the $[a(0)]_{m_sm_s'}$ and $[a(1)]_{m_sm_s'}$ amplitudes cannot be different from zero for the same pair of m_s,m_s' indices and

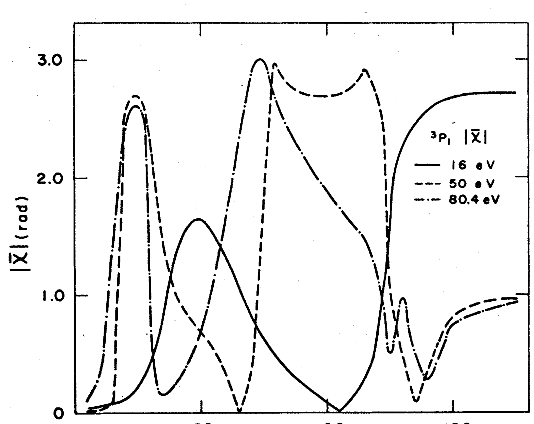

FIG. 2. $\bar{\chi}$ parameter for the $4s[\frac{3}{2}]_1^0(^3P_1)$ state.

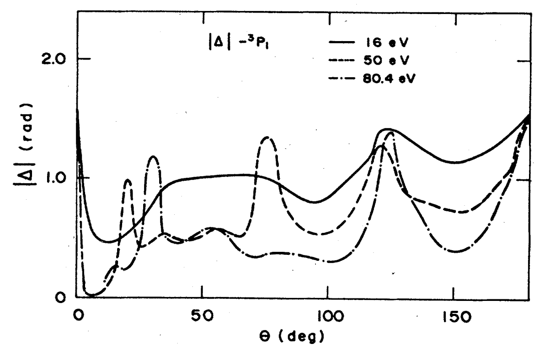

FIG. 3. Δ parameter for the $4s[\frac{3}{2}]_1^0(^3P_1)$ state.

therefore their product $[a(0)]_{m_sm_s'}[a(1)]_{m_sm_s'}$ is *always* zero for *any* pair of m_s,m_s' indices. Consequently their sum $\langle a(0)a(1)\rangle$ is also zero. The line of proof is identical for $\langle a(1)a(-1)\rangle=0$. The above proof was simplified by Blum and Kleinpoppen[53] by stating that for $\theta=0°$ and 180° cylindrical symmetry is restored to the radiating ensemble from which it immediately follows that the off-diagonal density-matrix elements will become zero.

A comment should be directed to angular or polarization-correlation experiments where only linear-polarization properties are studied.[33,34] In this case $\cos\Delta$ and $\cos\bar{\chi}$ are not measured separately, only their product

$$\cos\chi=\cos\Delta\cos\bar{\chi} \tag{32}$$

is. From Eqs. (26b) and (26c) it follows that

$$\cos\chi=\cos\Delta\cos\bar{\chi}=\frac{\mathrm{Re}\langle a(0)a(1)\rangle}{\sqrt{\sigma_0\sigma_1}}\ . \tag{33}$$

From our considerations it follows that at $\theta=0°$ and 180°, $\cos\chi=0$ also for spin-orbit-coupled systems. In the *LS*-coupling case $\cos\Delta\equiv1$ and χ goes to $\bar{\chi}$. However, at $\theta=0°$ the limit of χ is not necessarily zero.

The spin-orbit interaction also introduces interesting effects for Stokes and related parameters. In this case, P and μ are not equal to 1. In other words, the light beam is not polarized, and it is partially coherent. P and μ can be helpful in understanding the selection rule. At 0° and 180°, we can view the unpolarized emitted radiation as a superposition of polarized beams that are not coherent since $\mu=0$. We observe a spin-flip process only if the incident electron excites a state with $m_j=1$. Consequently,

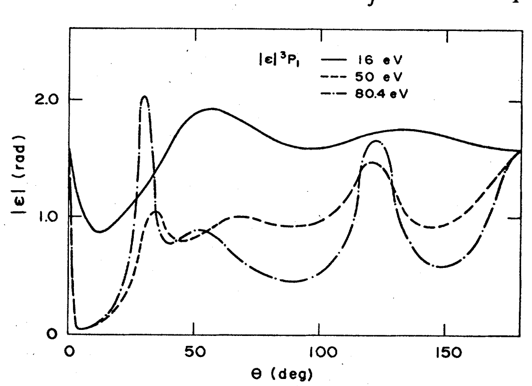

FIG. 4. ϵ parameter for the $4s[\frac{3}{2}]_1^0(^3P_1)$ state.

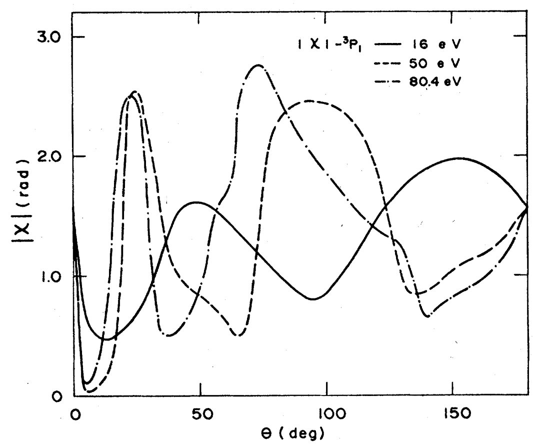

FIG. 5. χ parameter for the $4s[\frac{3}{2}]_1^0(^3P_1)$ state.

the light emitted by the deexcitation of both states with $m_j=0$ and 1 is incoherent. Threshold[8] and pseudothreshold experiments[11] lead to similar conclusions. According to McFarland and Mittleman,[67] in this case, the spin-flip process due to the spin-orbit interaction is responsible for the polarization being different from one.

We should add that the influence of the spin-flip process is more evident in μ than in P which can be quite close to one at 0°. For angles between 0° and 180°, an incident electron can excite both states with $m_j=0$ and 1, with or without spin flip. Thus, the emitted light will be partially coherent. At higher energies, the exchange process responsible for the spin flip decreases and μ should become closer to the value 1 of the LS-coupled cases.

IV. CALCULATIONS

We incorporated[59] the spin-orbit interaction in the excited state by a linear combination of singlet and triplet components in a way suggested by Cowan and Andrew,[68] and Cowan,[69] and McConnel and Moiseiwitsch:[70]

$$|4s'[\tfrac{1}{2}]_1^0\rangle = b\,|4^1P\rangle + a\,|4^3P\rangle\ , \tag{34}$$

and

$$|4s[\tfrac{3}{2}]_1^0\rangle = -a\,|4^1P\rangle + b\,|4^3P\rangle\ , \tag{35}$$

where $a=-0.450$ and $b=0.893$. The constants a and b were calculated by Cowan.[71] $|4^1P\rangle$ and $|4^3P\rangle$ refer to the LS-coupled states represented by the fixed-core Hartree-Fock wave functions. The same $4s$ orbital was used to construct the LS-coupled wave functions for both $[(3p^5)4s]4^3P$ and $[(3p^5)4s^1]4^1P$ configurations.

As in Ref. 59, we define the direct and exchange parts of the T matrices as

$$T^D_{LM_LS} = \int d\vec{r}_1 d\vec{r}_2 f^{(+)\mathrm{HF}}_{\vec{p}}(r_1)[f^{(-)\mathrm{HF}}_{\vec{q}}(r_1)]^* \times v(\vec{r}_1-\vec{r}_2)R_{3p}(r_2)R_{4s}(r_2) \times Y_{1M_L}(\hat{r}_2)Y_{00}(\hat{r}_2) \tag{36}$$

and

$$T^E_{LM_LS} = \int d\vec{r}_1 d\vec{r}_2 f^{(+)\mathrm{HF}}_{\vec{p}}(r_1)[f^{(-)\mathrm{HF}}_{\vec{q}}(r_2)]^* \times v(\vec{r}_1-\vec{r}_2)R_{3p}(r_1)R_{4s}(r_2) \times Y_{1M_L}(\hat{r}_1)Y_{00}(\hat{r}_2)\ , \tag{37}$$

where $f^{(+)\mathrm{HF}}_{\vec{p}}$ and $(f^{(-)\mathrm{HF}}_{\vec{q}})^*$ represent the incoming and outgoing electron with momenta $\vec{p}$ and $\vec{q}$, respectively. $R_{3p}(r)Y_{1M_L}(\hat{r})$ and $R_{4s}(r)Y_{00}(\hat{r})$ are normalized Hartree-Fock ground-state orbitals, with $Y_{LM_L}(\hat{r})$ denoting the spherical harmonics. $v(\vec{r}_1-\vec{r}_2)$ is the Coulomb potential.

From now on, we simplify our notation as

$$T^D_{L=(1,M_L),S=0} \rightarrow T^{SD}_M\ ,$$

$$T^E_{L=(1,M_L),S=0} \rightarrow T^{SE}_M\ ,$$

$$T^E_{L=(1,M_L),S=1} \rightarrow T^{TE}_M\ .$$

The differential cross sections for the excitation of the magnetic sublevels 0 and 1 can be written for the $4s[\frac{3}{2}]_1^0(^3P_1)$ state as

$$\sigma_0 = \frac{1}{4\pi^2}\frac{q}{p}\left[\frac{a^2}{2}|2T_0^{SD}-T_0^{SE}|^2+\frac{b^2}{2}|T_1^{TE}|^2\right]\ , \tag{38}$$

$$\sigma_1 = \frac{1}{4\pi^2}\frac{q}{p}\left[\frac{a^2}{2}|2T_1^{SD}-T_1^{SE}|^2+\frac{b^2}{4}|T_0^{TE}|^2 + \frac{b^2}{4}|T_1^{TE}|^2\right]\ . \tag{39}$$

TABLE XI. Comparison of theoretical and experimental results for λ and $\cos\chi$.

Angle (deg)	λ (singlet)	λ (triplet)	$\cos\chi$ (singlet)	$\cos\chi$ (triplet)	Reference
			Energy=50 eV		
5	0.72 ±0.01	0.60 ±0.05	0.55 ±0.16	0.63 ±0.06	Expt., Ref. 33
5	0.70	0.70	1.000	0.999	Present work
10	0.37 ±0.05	0.32 ±0.05	0.63 ±0.06	0.90 ±0.16	Expt., Ref. 34
10	0.33	0.33	0.999	0.997	Present work[a]
			Energy=80 eV		
10	0.26 ±0.05	0.25 ±0.05	0.55 ±0.06	0.96 ±0.06	Expt., Ref. 34
10	0.134	0.134	0.939	0.935	Present work[a]

[a]Theoretical results calculated for incident electron energy of 80.4 eV.

We can write the λ, $\mathcal{X}$, Δ, and ϵ parameters as functions of the T matrices, for the $4s[\frac{3}{2}]_1^0({}^3P_1)$ state:

$$\lambda=\frac{\sigma_0}{\sigma_0+2\sigma_1}\,, \tag{40}$$

$$\cos\Delta=\frac{\frac{1}{4}\pi^2\frac{q}{p}\left|\left[\frac{a^2}{2}(2T_0^{SD}-T_0^{SE})^*(2T_1^{SD}-T_1^{SE})-\frac{b^2}{4}T_0^{TE*}T_1^{TE}\right]\right|}{(\sigma_0\sigma_1)^{1/2}}\,, \tag{41}$$

$$\cos\mathcal{X}=\frac{\mathrm{Re}\left[\frac{a^2}{2}(2T_0^{SD}-T_0^{SE})^*(2T_1^{SD}-T_1^{SE})-\frac{b^2}{4}T_0^{TE*}T_1^{TE}\right]}{\left|\left[\frac{a^2}{2}(2T_0^{SD}-T_0^{SE})^*(2T_1^{SD}-T_1^{SE})-\frac{b^2}{4}T_0^{TE*}T_1^{TE}\right]\right|}\,, \tag{42}$$

and

$$\cos\epsilon=\frac{\frac{1}{4\pi^2}\frac{q}{p}\left[\frac{a^2}{2}\,|\,2T_1^{SD}-T_1^{SE}\,|^2-\frac{b^2}{4}\,|\,T_1^{TE}\,|^2\right]}{\sigma_1}\,. \tag{43}$$

For the state $4s'[\frac{1}{2}]_1^0({}^1P_1)$ the formulas are analogous with a and b interchanged.

V. RESULTS AND DISCUSSIONS

We calculated the parameters λ, $\overline{\mathcal{X}}$, Δ, ϵ, and $\mathcal{X}$ for the states $4s[\frac{3}{2}]_1^0({}^3P_1)$ and $4s'[\frac{1}{2}]_1^0({}^1P_1)$ of argon at the incident electron energies of 16, 20, 30, 50, and 80.4 eV. The results are shown in Tables I–X.

To visualize the general behavior of each parameter as a function of the energy, we plotted our results for the incident energies of 16, 50, and 80.4 eV (Figs. 1–5) for the $4s[\frac{3}{2}]_1^0({}^3P_1)$ state. The figures for the $4s'[\frac{1}{2}]_1^0({}^1P_1)$ state would be very similar to the ones presented, although the spin-orbit effect is weaker in this case.

Since the exchange parts of the T matrices become smaller for higher energies, the expressions for the coincidence parameters become strongly dominated by the ${}^1P_1$ component of the wave function [see Eqs. (37)–(40)]. Thus, as the energy increases, the parameters should approach the "LS-coupled" values. For the ϵ and Δ parameters the limit is zero and we can see in Figs. 3 and 4 how the curves show the expected behavior.

Two points in regard to the structures of the Δ and ϵ parameters deserve emphasis. First, the peaks for the forward and backward scattering are explained by the selection rule. Second, the structure in the intermediate angular region, even for higher energies, can often be explained in a way similar to the spin-polarization effect of Kessler.[72] The peaks usually occur in the minima of σ_0 (for Δ) and σ_1 (for ϵ and Δ), where the addition of a weak potential like the spin-orbit interaction can significantly change the spin orientation of the electron.

The evaluation of our results is limited by the lack of experimental data. The only two experimental papers[33,34] on the subject provide results for two angles at 50 eV and one angle at 80 eV (see comparison in Table XI). In addition, both angles 5° and 10° are in a region where the curves are very sharp. Due to the strong and abrupt structure of our parameters, we can be neither enthusiastic about the good agreement at some points nor pessimistic about the discrepancy at others. We hope that future experiments will provide a better test of our approximations.

ACKNOWLEDGMENTS

The authors gratefully acknowledge the joint support of the U.S.—Latin American Cooperative Science Program; National Science foundation (OIP) and Conselho Nacional de Pesquisas do Brasil (CNPq, Brazil) which made this research possible. One of us (F.J.d.P.) was a CNPq fellow. We thank L. A. Collins, B. I. Schneider, D. W. Norcross, D. C. Cartwright, and V. McKoy for valuable discussions.

*Present address: Joint Institute for Laboratory Astrophysics, University of Colorado and National Bureau of Standards, Boulder, CO 80309.

†Present address: Institute for Modern Optics, Department of Physics and Astronomy, University of New Mexico, Albuquerque, NM 87131.

[1]H. W. B. Skinner, Proc. R. Soc. London, Ser. A **112**, 642 (1926).

[2]H. W. B. Skinner and E. T. S. Appleyard, Proc. R. Soc. London, Ser. A **117**, 224 (1927).

[33]See review by K. Blum and H. Kleinpoppen, Phys. Rep. **52**, 203 (1979).

[4]J. R. Oppenheimer, Z. Phys. **43**, 27 (1927).

[5]J. R. Oppenheimer, Proc. Natl. Acad. Sci. USA **13**, 800 (1927).

[6]J. R. Oppenheimer, Phys. Rev. **32**, 231 (1932).

[7]W. G. Penney, Proc. Natl. Acad. Sci. USA **18**, 231 (1932).

[8]I. C. Percival and M. J. Seaton, Philos. Trans. R. Soc. London, Ser. A **251**, 113 (1958).

[9]J. Wykes, J. Phys. B **5**, 1126 (1972).

[10]R. E. Imhoff and F. H. Read, J. Phys. B **4**, 450 (1971).

[11]G. C. M. King, A. Adams, and F. H. Read, J. Phys. B **5**, L254 (1972).

[12]A. Pochat, D. Rozuel, and J. Peresse, J. Phys. (Paris) **34**, 701 (1973).

[13]K. Rubin, B. Bederson, M. Goldstein, and R. E. Collins, Phys. Rev. **182**, 201 (1969).

[14]J. Macek and D. H. Jaecks, Phys. Rev. A **4**, 2288 (1971).
[15]M. Eminyan, K. B. MacAdam, J. Slevin, and H. Kleinpoppen, Phys. Rev. Lett. **31**, 576 (1973).
[16]M. Eminyan, K. B. MacAdam, J. Slevin, and H. Kleinpoppen, J. Phys. B **7**, 1519 (1974).
[17]M. C. Standage and H. Kleinpoppen, Phys. Rev. Lett. **36**, 577 (1976).
[18]M. Eminyan, K. B. MacAdam, J. Slevin, M. C. Standage, and H. Kleinpoppen, J. Phys. B **8**, 2058 (1975).
[19]A. Ugbabe, P. J. C. Teubner, E. Weigold, and H. Arriola, J. Phys. B **10**, 71 (1977).
[20]K. H. Tan, J. Fryar, P. S. Farago, and J. W. McConkey, J. Phys. B **10**, 1073 (1977).
[21]V. C. Sutcliffe, G. N. Haddad, N. C. Steph, and D. E. Golden, Phys. Rev. A **17**, 100 (1978).
[22]M. T. Hollywood, A. Crowe, and J. F. Williams, J. Phys. B **12**, 819 (1979).
[23]N. C. Steph and D. E. Golden, Phys. Rev. A **21**, 759 (1980).
[24]N. C. Steph and D. E. Golden, Phys. Rev. A **21**, 1848 (1980).
[25]J. Selvin, H. I. Porter, M. Eminyan, A. Defrance, and G. Vassilev, J. Phys. B **13**, L23 (1980).
[26]R. McAdams, M. T. Hollywood, A. Crowe, and J. F. Williams, J. Phys. B **13**, 3691 (1980).
[27]J. Slevin, H. I. Porter, M. Eminyan, A. Defrance, and G. Vassilev, J. Phys. B **13**, 3009 (1980).
[28]A. Crowe, T. C. F. King, and J. F. Williams, J. Phys. B **14**, 1219 (1981).
[29]A. Crowe and J. C. Nogueira, J. Phys. B **15**, L501 (1982).
[30]A. Crowe, J. C. Nogueira, and Y. C. Liew, J. Phys. B **16**, 481 (1983).
[31]H. B. van Linden van der Heuvell, E. M. van Gasteren, J. van Eck, and H. G. M. Heideman, J. Phys. B **16**, 1619 (1983).
[32]H. Arriola, P. J. O. Teubner, A. Ugbabe, and E. Weigold, J. Phys. B **8**, 1275 (1975).
[33]I. C. Malcolm and J. W. McConkey, J. Phys. B **12**, 511 (1979).
[34]A. Pochat, F. Gelebart, and J. Peresse, J. Phys. B **13**, L79 (1980).
[35]H. Kleinpoppen and I. McGregor, in *Coherence and Correlation in Atomic Collisions,* edited by H. Kleinpoppen and J. F. Williams (Plenum, New York, 1980), p. 109.
[36]I. McGregor, D. Hils, R. Hippler, N. A. Malik, J. F. Williams, A. A. Zaidi, and H. Kleinpoppen, J. Phys. B **15**, L411 (1982).
[37]H. Nishimura, A. Danjo, Y. Koike, K. Kaui, H. Sugahara, and A. Takahashi, in Proceedings of the First U.S.-Japan Seminar on Electron Molecule Collisions and Photoionization Processes, Pasadena, California, 1982 (unpublished).
[38]A. Crowe, S. J. King, and P. A. Neil, in International Symposium on Polarization and Correlation in Electron-Atom Collisions, Munster, 1983 (unpublished); and private communication.
[39]A. A. Zaidi, I. McGregor, and H. Kleinpoppen, Phys. Rev. Lett. **45**, 1168 (1980).
[40]A. A. Zaidi, S. M. Khalid, I. McGregor, and H. Kleinpoppen, J. Phys. B **14**, L503 (1981).
[41]G. F. Hanne, K. Wemhoff, A. Wolcke, and J. Kessler, J. Phys. B **14**, L507 (1981).
[42]S. J. Buckman and P. J. O. Teubner, J. Phys. B **12**, 1741 (1979); H. W. Hermann, I. V. Hertel, and M. Kelley, *ibid.* **13**, 3465 (1980).
[43]J. F. Williams, in *The Physics of Electronic and Atomic Collisions,* Invited Lectures, Review Papers and Progress Reports of the Ninth Internation Conference on the Physics of Electronic and Atomic Collisions, Seattle, 1975, edited by J. Risley (University of Washington, Seattle, 1975), p. 139.
[44]P. G. O. Teubner, S. J. Buckman, and J. Furst, in *Abstracts of the Eleventh International Conference on the Physics of Electronic and Atomic Collisions, Kyoto, 1979,* edited by K. Takayanagi and N. Oda (The Society for Atomic Collision Research, Kyoto, 1979), p. 192.
[45]A. J. Dixon, S. T. Hood, and E. Weigold, Phys. Rev. Lett. **40**, 1262 (1978).
[46]S. T. Hood, E. Weigold, and A. J. Dixon, J. Phys. B **12**, 631 (1978).
[47]E. Weigold, L. Frost, and K. J. Nygaard, Phys. Rev. A **21**, 1950 (1980).
[48]J. F. Williams, J. Phys. B **14**, 1197 (1981).
[49]I. C. Malcolm and J. W. McConkey, J. Phys. B **12**, L67 (1979).
[50]K. Becker, H. W. Darren, and J. W. McConkey, J. Phys. B **16**, L177 (1983).
[51]J. W. McConkey, in *Symposium on Electron-Molecule Collisions, Invited Papers,* edited by S. Shimamura and M. Matsuzawa (University of Tokyo, Tokyo, 1979).
[52]U. Fano and J. Macek, Rev. Mod. Phys. **45**, 553 (1973). The analysis is also applied to hyperfine effects.
[53]See review by K. Blum and H. Kleinpoppen, in *Electron-Atom and Electron-Molecule Collisions,* edited by J. Hinze (Plenum, New York, 1980), p. 1, and references therein.
[54]See K. Blum, *Density Matrix Theory and Applications* (Plenum, New York, 1981), and references therein.
[55]K. Bartschat, K. Blum, G. F. Hanne, and J. Kessler, J. Phys. B **14**, 3761 (1981).
[56]J. Macek and I. V. Hertel, J. Phys. B **7**, 2173 (1974).
[57]F. J. da Paixão, N. Padial, Gy. Csanak, and K. Blum, Phys. Rev. Lett. **45**, 1164 (1980).
[58]Gy. Csanak, H. S. Taylor, and R. Yaris, Phys. Rev. A **3**, 1322 (1971).
[59]N. T. Padial, G. D. Meneses, F. J. da Paixão, Gy. Csanak, and D. C. Cartwright, Phys. Rev. A **23**, 2194 (1981).
[60]G. D. Meneses, N. T. Padial, and Gy. Csanak, J. Phys. B **11**, L237 (1978).
[61]L. E. Machado, E. P. Leal, and Gy. Csanak, J. Phys. B **15**, 1773 (1983).
[62]V. V. Balashov, E. G. Berezhko, N. M. Kabachnik, and A. I. Magunov, J. Phys. B **14**, 357 (1981).
[63]J. S. Briggs, J. H. Macek, and K. Taulbjerg, J. Phys. B **12**, 1457 (1979).
[64]Expression (10) also defines the density matrix $\rho_{mm'}$. Equation (8) shows that some relations among the elements of the density matrix can be obtained from the electron-photon coincidence parameters $O^{\rm col}_{1-}$, $A^{\rm col}_{0}$, $A^{\rm col}_{1+}$, and $A^{\rm col}_{2+}$. In some circumstances, these relations determine completely the density matrix as we can see in Ref. 4.
[65]M. Born and E. Wolf, *Principles of Optics,* 4th ed. (Pergamon, New York, 1970).
[66]See H. W. Hermann and I. V. Hertel, Comments At. Mol. Phys. **12**, 61 (1982).
[67]R. H. McFarland and M. H. Mittleman, Phys. Rev. Lett. **20**, 899 (1968).
[68]R. D. Cowan and K. L. Andrew, J. Opt. Soc. Am. **55**, 502 (1965).
[69]R. D. Cowan, J. Opt. Soc. Am. **58**, 808 (1968); **58**, 924 (1968).
[70]J. C. McConnel and B. L. Moiseiwitsch, J. Phys. B **1**, 406 (1968).
[71]R. D. Cowan (private communication).
[72]J. Kessler, Bull. Am. Phys. Soc. **13**, 98 (1968).